

# UPCommons

## Portal del coneixement obert de la UPC

<http://upcommons.upc.edu/e-prints>

This is a post-peer-review, pre-copyedit version of an article published in *Journal of Scientific Computing*. The final authenticated version is available online at: ><http://dx.doi.org/10.1007/s10915-018-0880-x>>

## Spectrally-consistent regularization of Navier–Stokes equations

F.X.Trias · D.Folch · A.Gorobets · A.Oliva

Received: date / Accepted: date

**Abstract** The incompressible Navier-Stokes equations form an excellent mathematical model for turbulent flows. However, direct simulations at high Reynolds numbers are not feasible because the convective term produces far too many relevant scales of motion. Therefore, in the foreseeable future, numerical simulations of turbulent flows will have to resort to models of the small scales. Large-eddy simulation (LES) and regularization models are examples thereof. In the present work, we propose to combine both approaches in a spectrally-consistent way: *i.e.* preserving the (skew-)symmetries of the differential operators. Restoring the Galilean invariance of the regularization method results into an additional hyperviscosity term. In this way, the convective production of small scales is effectively restrained whereas the destruction of the small scales is enhanced by this hyperviscosity effect. This approach leads to a blending between regularization of the convective term and LES. The performance of these improvements is assessed through application to Burgers' equation, homogeneous isotropic turbulence and a turbulent channel flow.

**Keywords** regularization · Navier–Stokes · LES · turbulence

**PACS** 47.10.ad · 47.27.ep · 47.27.Gs · 47.27.nd

**Mathematics Subject Classification (2000)** 76F65 · 76F05 · 76D05

---

F.X.Trias, D.Folch, A.Oliva  
Heat and Mass Transfer Technological Center, Technical University of Catalonia, ETSEIAT,  
c/Colom 11, 08222 Terrassa, Spain  
E-mail: xavi@cttc.upc.edu,davidf@cttc.upc.edu,oliva@cttc.upc.edu

A.Gorobets  
Keldysh Institute of Applied Mathematics, 4A, Miusskaya Sq., Moscow 125047, Russia

## 1 Introduction

The incompressible Navier–Stokes (NS) equations form an excellent mathematical model for turbulent flows. In primitive variables they read

$$\partial_t \mathbf{u} + \mathcal{C}(\mathbf{u}, \mathbf{u}) = \mathcal{D}\mathbf{u} - \nabla p; \quad \nabla \cdot \mathbf{u} = 0, \quad (1)$$

where  $\mathbf{u}$  denotes the velocity field,  $p$  represents the pressure, the non-linear convective term is defined by  $\mathcal{C}(\mathbf{u}, \mathbf{v}) = (\mathbf{u} \cdot \nabla)\mathbf{v}$ , and the diffusive term reads  $\mathcal{D}\mathbf{u} = \nu \Delta \mathbf{u}$ , where  $\nu$  is the kinematic viscosity.

Preserving the symmetries of the continuous differential operators at discrete level has been shown to be a very suitable approach for direct numerical simulation (DNS) (see the work by Verstappen and Veldman [41] or the more recent review by Perot [25], for example). Doing so, certain fundamental properties such as the inviscid invariants - kinetic energy, enstrophy (in 2D) and helicity (in 3D) - are exactly preserved in a discrete sense. However, direct simulations at high Reynolds numbers are not feasible because the convective term produces far too many relevant scales of motion. Therefore, a dynamically less complex mathematical formulation is needed. In the quest for such a formulation, we consider regularizations [17,12,18] of the nonlinearity. The first outstanding approach in this direction goes back to Leray [20]. In this regard, simulations using the Leray- $\alpha$  model can be found in many works [6,28,13,24,29,15,26]. The Navier–Stokes- $\alpha$  model also forms an example of regularization modeling (see the works [10,12,16], for instance). The regularization methods basically alter the convective terms to reduce the production of small scales of motion. In doing so, Verstappen [38] proposed to preserve exactly the symmetry and conservation properties of the convective terms. This requirement yielded a family of *symmetry-preserving regularization* models: a novel class of regularizations that restrains the convective production of smaller and smaller scales of motion in an unconditionally stable manner, meaning that the velocity cannot blow up in the energy-norm (in 2D also: enstrophy-norm). In our previous works [37,36,33], we restrict ourselves to the  $\mathcal{C}_4$  approximation: the convective term in the NS equations (1) is then replaced by the following  $\mathcal{O}(\epsilon^4)$ -accurate smooth approximation  $\mathcal{C}_4(\mathbf{u}, \mathbf{v})$  given by

$$\mathcal{C}_4(\mathbf{u}, \mathbf{v}) = \mathcal{C}(\bar{\mathbf{u}}, \bar{\mathbf{v}}) + \overline{\mathcal{C}(\bar{\mathbf{u}}, \mathbf{v}')} + \overline{\mathcal{C}(\mathbf{u}', \bar{\mathbf{v}})}, \quad (2)$$

where the prime indicates the residual of the filter, *e.g.*  $\mathbf{u}' = \mathbf{u} - \bar{\mathbf{u}}$ , which can be explicitly evaluated, and  $\overline{(\cdot)}$  represents a self-adjoint linear filter with filter length  $\epsilon$  that commutes with differential operators. Therefore, the governing equations result in

$$\partial_t \mathbf{u}_\epsilon + \mathcal{C}_4(\mathbf{u}_\epsilon, \mathbf{u}_\epsilon) = \mathcal{D}\mathbf{u}_\epsilon - \nabla p_\epsilon; \quad \nabla \cdot \mathbf{u}_\epsilon = 0, \quad (3)$$

where the variable names are changed from  $\mathbf{u}$  and  $p$  to  $\mathbf{u}_\epsilon$  and  $p_\epsilon$ , respectively, to stress that the solution of (3) differs from that of (1). Note that the  $\mathcal{C}_4$  approximation is also a skew-symmetric operator like the original convective operator. Hence, the same inviscid invariants as the original NS equations are preserved for the new set of PDEs (3). In this paper, regularizations of the NS equations that preserve this fundamental property are called *spectrally-consistent*. Similarly, we also call a discretization of the NS equations *spectrally-consistent* when the discrete representation of the (skew-)symmetric differential operators are given by a matrix which is spectrally equivalent: *e.g.* the skew-symmetric convective operator is

given by a skew-symmetric matrix, whereas the symmetric diffusive operator is represented by a symmetric matrix. From a physical point-of-view, this implies that the discrete convective terms redistributes energy over the scales of motion without dissipating it and the spatial discretization of diffusion dissipates energy from a scale without transporting energy to other scales of motion [35]. The  $\mathcal{C}_4$  regularization method has already been applied to several configurations [38, 37]. However, two main drawbacks have been observed: (i) due to the energy conservation, the model solution tends to display an additional hump in the tail of the spectrum and (ii) for very coarse meshes very stringent conditions are required for the linear filter.

In this context, here we propose to alter diffusion term in the same vein as convection. In Section 2, this new regularization method is presented and discussed. Firstly, a family of fourth-order accurate regularizations of convective term is obtained. Then, the modification of the linear diffusive operator follows from (approximately) restoring the Galilean invariance of the regularized equations. The modified diffusive term introduces an hyperviscosity effect and consequently enhances the destruction of small scales. Then, the only additional ingredient is a self-adjoint linear filter whose local filter length is determined from the criterion proposed in [33], *i.e.* the vortex-stretching mechanism must be stopped at the smallest grid scale. Furthermore, a blending between regularization modeling and Large-Eddy Simulation (LES) is proposed. This is addressed in Section 3. The performance of the proposed method is assessed through application to a 1D Burgers' equation, homogeneous isotropic turbulence and a turbulent channel flow in Section 4. Finally, relevant results are summarized and conclusions are given.

## 2 Spectrally-consistent regularization of the Navier–Stokes equations

### 2.1 Symmetries and conservation properties

For convenience, we firstly introduce the following notation:

$$d(\mathbf{u}, \mathbf{v}) = (\mathbf{u}, \mathcal{D}\mathbf{v}) \quad \text{and} \quad c(\mathbf{u}, \mathbf{v}, \mathbf{w}) = (\mathcal{C}(\mathbf{u}, \mathbf{v}), \mathbf{w}), \quad (4)$$

where the inner-product of functions is defined in the usual way:  $(a, b) = \int_{\Omega} a \cdot b d\Omega$ . The bi-linear operator  $d(\mathbf{u}, \mathbf{v})$  satisfies the following properties

$$d(\mathbf{u}, \mathbf{v}) = d(\mathbf{v}, \mathbf{u}) \quad \text{and} \quad d(\mathbf{u}, \mathbf{u}) < 0, \quad (5)$$

whereas the tri-linear form  $c(\mathbf{u}, \mathbf{v}, \mathbf{w})$  satisfies two fundamental symmetry properties

$$c(\mathbf{u}, \mathbf{v}, \mathbf{w}) = -c(\mathbf{u}, \mathbf{w}, \mathbf{v}) \quad \text{if} \quad \nabla \cdot \mathbf{u} = 0, \quad (6)$$

$$c(\mathbf{u}, \mathbf{v}, \Delta\mathbf{v}) = c(\Delta\mathbf{v}, \mathbf{v}, \mathbf{u}) \quad \text{in 2D}, \quad (7)$$

provided that the contribution of boundaries vanishes. These properties are extensively used to prove the conservation properties of the inviscid invariants of the original NS equations. Namely, the skew-symmetry (6) ensures the conservation of kinetic energy,  $1/2(\mathbf{u}, \mathbf{u})$ , and helicity,  $(\mathbf{u}, \boldsymbol{\omega})$ , where  $\boldsymbol{\omega} = \nabla \times \mathbf{u}$  is the vorticity. The enstrophy,  $1/2(\boldsymbol{\omega}, \boldsymbol{\omega})$ , also forms an inviscid invariant in the case of 2D flows. Actually, the stronger form of enstrophy invariance given by Eq.(7) also holds for the NS equations. For details the reader is referred to [17], for instance.

## 2.2 $\{\mathcal{CD}\}_4^\gamma$ regularization modeling

Regularization aims to modify the convective term in such a way that a dynamically less complex mathematical formulation results. Let us assume that we have a self-adjoint linear filter  $(\bar{\cdot}) : \mathbf{u} \rightarrow \bar{\mathbf{u}}$  with the requirements that it filters out high frequency components and it commutes with differential operators. Now, for convenience, let us define the following conditional function

$$\varphi_i(\mathbf{u}) = \begin{cases} \mathbf{u}, & \text{if } i = 0 \\ \bar{\mathbf{u}}, & \text{if } i = 1 \end{cases} \quad (8)$$

Then, a family of modified (regularized) non-linear operators can be easily constructed

$$\tilde{\mathcal{C}}(\mathbf{u}, \mathbf{v}) = \sum_{i,j,k=0}^1 a_{ijk} \tilde{\mathcal{C}}_{ijk}(\mathbf{u}, \mathbf{v}), \quad (9)$$

where  $\tilde{\mathcal{C}}_{ijk}(\mathbf{u}, \mathbf{v}) = \varphi_k(\mathcal{C}(\varphi_i(\mathbf{u}), \varphi_j(\mathbf{v})))$ . Hence, regularization  $\tilde{\mathcal{C}}(\mathbf{u}, \mathbf{v})$  results into a linear combination of (up to) eight terms. Among all the possible combinations we find the regularization proposed by Leray [20],  $a_{100} = 1$  (with the rest of  $a_{ijk} = 0$ ). Firstly, the equality  $\sum_{i,j,k=0}^1 a_{ijk} = 1$  must be satisfied to guarantee that  $\tilde{\mathcal{C}}(\mathbf{u}, \mathbf{v}) \approx \mathcal{C}(\mathbf{u}, \mathbf{v}) + \mathcal{O}(\epsilon^n)$  with  $n \geq 2$ . Then, several restrictions can be applied to the coefficients  $a_{ijk}$ . Namely,

$$a_{ijk} = a_{ikj} \quad \text{and} \quad a_{ijk} = a_{jik}, \quad (10)$$

where the latter ensures that the skew-symmetry property (6) is exactly preserved whereas the former is needed to guarantee that the form of vorticity transport equation is not altered. They impose four additional restrictions to the coefficients  $a_{ijk}$  and lead to a family of second-order accurate regularization models. Among them, we find the second-order approximation proposed by Verstappen [38],

$$\mathcal{C}_2(\mathbf{u}, \mathbf{v}) = \tilde{\mathcal{C}}_{111}(\mathbf{u}, \mathbf{v}) = \overline{\mathcal{C}(\bar{\mathbf{u}}, \bar{\mathbf{v}})}. \quad (11)$$

It must be noticed that the following restriction

$$a_{ijk} = a_{kji}, \quad (12)$$

is needed to preserve the strong form of the enstrophy invariance (7) and follows automatically from the restriction given in (10). Then, to cancel second-order terms three additional conditions must be imposed:

$$\sum_{j,k=0}^1 a_{1jk} = 0 \quad \sum_{i,k=0}^1 a_{i1k} = 0 \quad \sum_{i,j=0}^1 a_{ij1} = 0. \quad (13)$$

Finally, without the loss of generality we can restrict ourselves to solutions where  $a_{000} = 0$ . This leads to a family of fourth-order accurate regularization methods

$$\mathcal{C}_4^\gamma(\mathbf{u}, \mathbf{v}) = \mathcal{C}_4^0(\mathbf{u}, \mathbf{v}) + \gamma \mathcal{E}_4(\mathbf{u}, \mathbf{v}), \quad (14)$$

where

$$\mathcal{C}_4^0(\mathbf{u}, \mathbf{v}) = \frac{1}{2} (\tilde{\mathcal{C}}_{001} + \tilde{\mathcal{C}}_{010} + \tilde{\mathcal{C}}_{100} - \tilde{\mathcal{C}}_{111}) (\mathbf{u}, \mathbf{v}), \quad (15)$$

$$\mathcal{E}_4(\mathbf{u}, \mathbf{v}) = (\tilde{\mathcal{C}}_{011} + \tilde{\mathcal{C}}_{101} + \tilde{\mathcal{C}}_{110}) (\mathbf{u}, \mathbf{v}) - \frac{1}{2} (\tilde{\mathcal{C}}_{001} + \tilde{\mathcal{C}}_{010} + \tilde{\mathcal{C}}_{100} + 3\tilde{\mathcal{C}}_{111}) (\mathbf{u}, \mathbf{v}). \quad (16)$$

Note that  $\mathcal{C}_4^0(\mathbf{u}, \mathbf{v}) = \mathcal{C}(\mathbf{u}, \mathbf{v}) + \mathcal{O}(\epsilon^4)$  whereas  $\mathcal{E}_4(\mathbf{u}, \mathbf{v}) = \mathcal{O}(\epsilon^4)$ . Even more importantly,

$$\mathcal{C}_4^\gamma(\mathbf{u}, \mathbf{v}) = \mathcal{C}(\mathbf{u}, \mathbf{v}) + (\gamma + 1)\mathcal{O}(\epsilon^4) + \mathcal{O}(\epsilon^6). \quad (17)$$

Therefore,  $\mathcal{C}_4^\gamma$  is fourth-order accurate except for  $\gamma = -1$  that becomes sixth-order. Actually for  $\gamma = 1$  and  $\gamma = -1$ ,  $\mathcal{C}_4^\gamma$  becomes the  $\mathcal{C}_4$  and  $\mathcal{C}_6$  approximations proposed by Verstappen [38],

$$\mathcal{C}_4(\mathbf{u}, \mathbf{v}) = \mathcal{C}_4^{\gamma=1}(\mathbf{u}, \mathbf{v}) = \mathcal{C}(\bar{\mathbf{u}}, \bar{\mathbf{v}}) + \overline{\mathcal{C}(\bar{\mathbf{u}}, \mathbf{v}')} + \overline{\mathcal{C}(\mathbf{u}', \bar{\mathbf{v}})}, \quad (18)$$

$$\mathcal{C}_6(\mathbf{u}, \mathbf{v}) = \mathcal{C}_4^{\gamma=-1}(\mathbf{u}, \mathbf{v}) = \mathcal{C}(\bar{\mathbf{u}}, \bar{\mathbf{v}}) + \mathcal{C}(\bar{\mathbf{u}}, \mathbf{v}') + \mathcal{C}(\mathbf{u}', \bar{\mathbf{v}}) + \overline{\mathcal{C}(\mathbf{u}', \mathbf{v}')}, \quad (19)$$

respectively. Notice that the  $\mathcal{C}_4^\gamma$  regularization can also be viewed as a linear combination of  $\mathcal{C}_4$  and  $\mathcal{C}_6$

$$\mathcal{C}_4^\gamma(\mathbf{u}, \mathbf{v}) = \frac{1}{2} ((\mathcal{C}_4 + \mathcal{C}_6) + \gamma(\mathcal{C}_4 - \mathcal{C}_6))(\mathbf{u}, \mathbf{v}). \quad (20)$$

The approximations  $\mathcal{C}_4^\gamma$  maintains all the invariant transformations of the NS equations, except, in general, the Galilean transformation. These transformations are listed in [27], for instance. To restore the Galilean invariance we need to replace the time-derivative,  $\partial_t \mathbf{u}_\epsilon$ , by the following forth-order approximation:

$$(\partial_t)_4^\gamma \mathbf{u}_\epsilon = \partial_t (\mathbf{u}_\epsilon - 1/2(1 + \gamma)\mathbf{u}_\epsilon'') = \mathcal{G}_4^\gamma(\partial_t \mathbf{u}_\epsilon), \quad (21)$$

where  $\mathcal{G}_4^\gamma(\phi) = \phi - 1/2(1 + \gamma)\phi''$ . Here, the double prime indicates the residual of the residual of the filter, *i.e.*  $\mathbf{u}'' = (\mathbf{u}')' = \mathbf{u}' - \bar{\mathbf{u}}'$ . In this case, the new set of PDEs reads

$$(\partial_t)_4^\gamma \mathbf{u}_\epsilon + \mathcal{C}_4^\gamma(\mathbf{u}_\epsilon, \mathbf{u}_\epsilon) = \mathcal{D}\mathbf{u}_\epsilon - \nabla p_\epsilon; \quad \nabla \cdot \mathbf{u}_\epsilon = 0. \quad (22)$$

Therefore, Galilean invariance of  $\mathcal{C}_4^\gamma$  in Eq.(20) can be restored without modifying the time-derivative by simply setting  $\gamma = -1$ . However, it can be shown that such an approach has several drawbacks (read the first paragraph in Section 3.3). Another possibility relies on modifying appropriately other terms, *e.g.* the viscous dissipation. The total kinetic energy equation for (22) becomes

$$\frac{d}{dt} (\|\mathbf{u}_\epsilon\|^2 - 1/2(1 + \gamma)\|\mathbf{u}_\epsilon'\|^2) = (\mathbf{u}_\epsilon, \mathcal{D}\mathbf{u}_\epsilon) < 0, \quad (23)$$

provided that the filter is self-adjoint and  $\|\mathbf{u}\|^2 = (\mathbf{u}, \mathbf{u})$ . Therefore, modification of the time-derivative term (21) constitutes a dissipation model. Recalling that  $(\mathcal{G}_4^\gamma)^{-1}(\phi) \approx 2\phi - \mathcal{G}_4^\gamma(\phi) + \mathcal{O}(\epsilon^6)$ , we can obtain an energetically almost equivalent set of equations by modifying the viscous diffusive term

$$\partial_t \mathbf{u}_\epsilon + \mathcal{C}_4^\gamma(\mathbf{u}_\epsilon, \mathbf{u}_\epsilon) = \mathcal{D}_4^\gamma \mathbf{u}_\epsilon - \nabla p_\epsilon; \quad \nabla \cdot \mathbf{u}_\epsilon = 0, \quad (24)$$

where the linear operator  $\mathcal{D}_4^\gamma \mathbf{u}$  is given by

$$\mathcal{D}_4^\gamma \mathbf{u} = \mathcal{D}\mathbf{u} + 1/2(1 + \gamma)(\mathcal{D}\mathbf{u}')'. \quad (25)$$

In this way, we are reinforcing the dissipation at the smallest grid scales. At this point, there are two parameters that need to be determined; namely, the constant  $\gamma$  and the local filter length,  $\epsilon$ . The former will determine the exact form of the regularization model whereas the latter will define the convolution kernel of the linear filter. These two issues are addressed in the following sections.

### 3 Restraining the production of small scales of motion

#### 3.1 Interscale interactions

To study the interscale interactions in more detail, we continue in the spectral space. The spectral representation of the convective term in the NS equations is given by

$$\mathcal{C}(\mathbf{u}, \mathbf{u})_{\mathbf{k}} = i\Pi(\mathbf{k}) \sum_{\mathbf{p}+\mathbf{q}=\mathbf{k}} \hat{\mathbf{u}}_{\mathbf{p}}\mathbf{q}\hat{\mathbf{u}}_{\mathbf{q}}, \quad (26)$$

where  $\Pi(\mathbf{k}) = I - \mathbf{k}\mathbf{k}^T/|\mathbf{k}|^2$  denotes the projector onto divergence-free velocity fields in the spectral space. Taking the Fourier transform of Eqs.(24), we obtain the evolution of each Fourier-mode  $\hat{\mathbf{u}}_{\mathbf{k}}(t)$  of  $\mathbf{u}_{\epsilon}(t)$  for the  $\{\mathcal{CD}\}_4^{\gamma}$  approximation

$$\left(\frac{d}{dt} + h_4^{\gamma}(\widehat{G}_{\mathbf{k}})\nu|\mathbf{k}|^2\right)\hat{\mathbf{u}}_{\mathbf{k}} + i\Pi(\mathbf{k}) \sum_{\mathbf{p}+\mathbf{q}=\mathbf{k}} f_4^{\gamma}(\widehat{G}_{\mathbf{k}}, \widehat{G}_{\mathbf{p}}, \widehat{G}_{\mathbf{q}})\hat{\mathbf{u}}_{\mathbf{p}}\mathbf{q}\hat{\mathbf{u}}_{\mathbf{q}} = \mathbf{F}_{\mathbf{k}}, \quad (27)$$

where  $\widehat{G}_{\mathbf{k}}$  denotes the  $\mathbf{k}$ -th Fourier-mode of the kernel of the convolution filter, *i.e.*,  $\widehat{\mathbf{u}}_{\mathbf{k}} = \widehat{G}_{\mathbf{k}}\hat{\mathbf{u}}_{\mathbf{k}}$ . Notice that hereafter, for simplicity, the subindex  $\epsilon$  is dropped. The mode  $\hat{\mathbf{u}}_{\mathbf{k}}$  interacts only with those modes whose wavevectors  $\mathbf{p}$  and  $\mathbf{q}$  form a triangle with the vector  $\mathbf{k}$ . Thus, compared with Eq.(26), every triadic interaction is multiplied by

$$f_4^{\gamma}(\widehat{G}_{\mathbf{k}}, \widehat{G}_{\mathbf{p}}, \widehat{G}_{\mathbf{q}}) = \frac{1}{2} \{(1 + \gamma)f_4 + (1 - \gamma)f_6\}(\widehat{G}_{\mathbf{k}}, \widehat{G}_{\mathbf{p}}, \widehat{G}_{\mathbf{q}}), \quad (28)$$

where the  $f_4$  and  $f_6$  are given by

$$f_4(\widehat{G}_{\mathbf{k}}, \widehat{G}_{\mathbf{p}}, \widehat{G}_{\mathbf{q}}) = \widehat{G}_{\mathbf{k}}\widehat{G}_{\mathbf{p}} + \widehat{G}_{\mathbf{k}}\widehat{G}_{\mathbf{q}} + \widehat{G}_{\mathbf{p}}\widehat{G}_{\mathbf{q}} - 2\widehat{G}_{\mathbf{k}}\widehat{G}_{\mathbf{p}}\widehat{G}_{\mathbf{q}}, \quad (29)$$

$$f_6(\widehat{G}_{\mathbf{k}}, \widehat{G}_{\mathbf{p}}, \widehat{G}_{\mathbf{q}}) = 1 - (1 - \widehat{G}_{\mathbf{k}})(1 - \widehat{G}_{\mathbf{p}})(1 - \widehat{G}_{\mathbf{q}}), \quad (30)$$

where  $0 < f_n \leq 1$  ( $n = 4, 6$ ). On the other hand, the  $\mathbf{k}$ -th Fourier mode of the diffusive term is multiplied by

$$h_4^{\gamma}(\widehat{G}_{\mathbf{k}}) = 1 + 1/2(1 + \gamma)(1 - \widehat{G}_{\mathbf{k}})^2, \quad (31)$$

where  $h_4^{\gamma} \geq 1$ . Moreover, since for a generic symmetric convolution filter (see [3], for instance),  $\widehat{G}_{\mathbf{k}} = 1 - \alpha^2|\mathbf{k}|^2 + \mathcal{O}(\alpha^4)$  with  $\alpha^2 = \epsilon^2/24$ , the functions  $f_4^{\gamma}$  and  $h_4^{\gamma}$  can be approximated by  $f_4^{\gamma} \approx 1 - 1/2(1 + \gamma)\alpha^4(|\mathbf{k}|^2|\mathbf{p}|^2 + |\mathbf{k}|^2|\mathbf{q}|^2 + |\mathbf{p}|^2|\mathbf{q}|^2)$  and  $h_4^{\gamma} \approx 1 + 1/2(1 + \gamma)\alpha^4|\mathbf{k}|^4$ , respectively. Therefore, the interactions between large scales of motion ( $\epsilon|\mathbf{k}| < 1$ ) approximate the NS dynamics up to  $\mathcal{O}(\epsilon^4)$ . Hence, the triadic interactions between large scales are only slightly altered. All the interactions involving longer wavevectors (smaller scales of motion) are reduced. The amount by which the interactions between the wavevector-triple  $(\mathbf{k}, \mathbf{p}, \mathbf{q})$  are lessened depends on the length of the legs of the triangle  $\mathbf{k} = \mathbf{p} + \mathbf{q}$ . For example,

all triadic interactions for which at least two legs are (much) longer than  $1/\epsilon$  are (strongly) attenuated; whereas, interactions for which at least two legs are (much) shorter than  $1/\epsilon$  are reduced to a small degree only. Interactions between the small scales of motion cannot be analyzed without knowing the exact transfer function of the filter since higher order terms may play an important role.

### 3.2 Stopping the vortex-stretching mechanism

Taking the curl of Eq.(24) leads to

$$\partial_t \boldsymbol{\omega} + \mathcal{C}_4^\gamma(\mathbf{u}, \boldsymbol{\omega}) = \mathcal{C}_4^\gamma(\boldsymbol{\omega}, \mathbf{u}) + \mathcal{D}_4^\gamma \boldsymbol{\omega}. \quad (32)$$

This equation resembles the vorticity equation that results from the NS equations: the only difference is that  $\mathcal{C}$  and  $\mathcal{D}$  are replaced by their regularizations  $\mathcal{C}_4^\gamma$  and  $\mathcal{D}_4^\gamma$ , respectively. If it happens that the vortex stretching term,  $\mathcal{C}_4^\gamma(\boldsymbol{\omega}, \mathbf{u})$ , in Eq.(32) is so strong that the dissipative term,  $\mathcal{D}_4^\gamma \boldsymbol{\omega}$ , cannot prevent the intensification of vorticity, smaller vortical structures are produced. Left-multiplying the vorticity transport Eq.(32) by  $\boldsymbol{\omega}$ , we can obtain the evolution of  $|\boldsymbol{\omega}|^2$ . In this way, the vortex-stretching and dissipation term contributions to  $\partial_t |\boldsymbol{\omega}|^2$  result

$$\boldsymbol{\omega} \cdot \mathcal{C}_4^\gamma(\boldsymbol{\omega}, \mathbf{u}) \quad \text{and} \quad \boldsymbol{\omega} \cdot \mathcal{D}_4^\gamma \boldsymbol{\omega}, \quad (33)$$

respectively. In order to prevent local intensification of vorticity, dissipation must dominate the vortex-stretching term contribution at the smallest grid scale,  $\mathbf{k}_c$ . In spectral space, this requirement leads to the following inequality

$$\frac{1}{2} \frac{\left( \hat{\boldsymbol{\omega}}_{\mathbf{k}_c} \cdot \mathcal{C}_4^\gamma(\boldsymbol{\omega}, \mathbf{u})_{\mathbf{k}_c}^* + \mathcal{C}_4^\gamma(\boldsymbol{\omega}, \mathbf{u})_{\mathbf{k}_c} \cdot \hat{\boldsymbol{\omega}}_{\mathbf{k}_c}^* \right)}{\hat{\boldsymbol{\omega}}_{\mathbf{k}_c} \cdot \hat{\boldsymbol{\omega}}_{\mathbf{k}_c}^*} \leq h_4^\gamma(\hat{G}_{\mathbf{k}_c}) \nu \mathbf{k}_c^2, \quad (34)$$

where  $(\cdot)^*$  represents the complex conjugate and the vortex-stretching term,  $\mathcal{C}_4^\gamma(\boldsymbol{\omega}, \mathbf{u})_{\mathbf{k}_c}$ , is given by

$$\mathcal{C}_4^\gamma(\boldsymbol{\omega}, \mathbf{u})_{\mathbf{k}_c} = \sum_{\mathbf{p}+\mathbf{q}=\mathbf{k}_c} f_4^\gamma(\hat{G}_{\mathbf{k}_c}, \hat{G}_{\mathbf{p}}, \hat{G}_{\mathbf{q}}) \hat{\boldsymbol{\omega}}_{\mathbf{p}} i \mathbf{q} \hat{\mathbf{u}}_{\mathbf{q}}. \quad (35)$$

Note that  $f_4^\gamma(\hat{G}_{\mathbf{k}_c}, \hat{G}_{\mathbf{p}}, \hat{G}_{\mathbf{q}})$  depends on the filter length  $\epsilon$  and, in general, on the wavevectors  $\mathbf{p}$  and  $\mathbf{q} = \mathbf{k}_c - \mathbf{p}$ . This makes very difficult to control the damping effect because  $f_4^\gamma$  cannot be taken out of the summation in (35). To avoid this, filters should be constructed from the requirement that the damping effect of all the triadic interactions at the smallest scale must be virtually independent of the interacting pairs, *i.e.*

$$f_4^\gamma(\hat{G}_{\mathbf{k}_c}, \hat{G}_{\mathbf{p}}, \hat{G}_{\mathbf{q}}) \approx f_4^\gamma(\hat{G}_{\mathbf{k}_c}). \quad (36)$$

This is a crucial property to control the subtle balance between convection and diffusion in order to stop the vortex-stretching mechanism. This point was addressed in detail in [36] where discrete linear filters were constructed to minimize the bandwidth of  $f_4^\gamma$ . Shortly, discrete linear filters,  $F$ , originally proposed in [36] are based on polynomial functions of the discrete diffusive operator,  $D$ ,

$$F = I + \sum_{m=1}^{\mathcal{M}} d_m D^m, \quad (37)$$

where the boundary conditions that supplement the NS equations are applied in Eq.(37) too. Here, we restrict ourselves to the case with  $\mathcal{M} = 2$  because it offers a good compromise between accuracy and computational cost [33]. In this case, the set of coefficients  $\{d_1, d_2\}$  that minimizes the bandwidth of  $f_4$  are given by

$$d_1 = -\frac{\widehat{G}_{\mathbf{k}_c} - 1}{2(2\widehat{G}_{\mathbf{k}_c} + 1)} \quad d_2 = \frac{2\widehat{G}_{\mathbf{k}_c}^2 - 3\widehat{G}_{\mathbf{k}_c} + 1}{16(2\widehat{G}_{\mathbf{k}_c} + 1)} \quad \text{if } 0 \leq \widehat{G}_{\mathbf{k}_c} < 1/2, \quad (38)$$

$$d_1 = \frac{1}{4} - \frac{\widehat{G}_{\mathbf{k}_c}}{4} \quad d_2 = 0 \quad \text{if } 1/2 \leq \widehat{G}_{\mathbf{k}_c} \leq 1, \quad (39)$$

and the corresponding transfer function of the filter,  $F$ , when using the classical 3-point approximation for the diffusive operator,  $D$ , is displayed in Figure 1 (top) for different values of  $\widehat{G}_{\mathbf{k}_c}$ . Figure 1 (bottom) shows the bandwidth of  $f_4^{5p}(\widehat{G}_{\mathbf{k}_c}, q)$  when using this 5-point filter. Notice that  $f_4^{5p}$  is bounded by  $q = 0$  and  $q = \mathbf{k}_c/2$ . The bandwidth is (very) small for the whole range  $0 \leq \widehat{G}_{\mathbf{k}_c} \leq 1$ ; therefore,  $f_4^{5p}$  satisfies the condition given in Eq.(36).

Then, the overall damping effect at the smallest grid scale,  $H_4(\widehat{G}_{\mathbf{k}_c})$ , follows straightforwardly

$$H_4(\widehat{G}_{\mathbf{k}_c}) = \frac{f_4^\gamma(\widehat{G}_{\mathbf{k}_c})}{h_4^\gamma(\widehat{G}_{\mathbf{k}_c})} = \frac{2\nu\mathbf{k}_c^2 \hat{\omega}_{\mathbf{k}_c} \cdot \hat{\omega}_{\mathbf{k}_c}^*}{\hat{\omega}_{\mathbf{k}_c} \cdot \mathcal{C}(\boldsymbol{\omega}, \mathbf{u})_{\mathbf{k}_c}^* + \mathcal{C}(\boldsymbol{\omega}, \mathbf{u})_{\mathbf{k}_c} \cdot \hat{\omega}_{\mathbf{k}_c}^*}, \quad (40)$$

with the condition that  $0 < H_4(\widehat{G}_{\mathbf{k}_c}) \leq 1$ . Notice that using Eqs.(28) and (31) and the definitions of  $f_4$  and  $f_6$  respectively given in Eqs.(29) and (30), and assuming that Eq.(36) is satisfied, we obtain  $h_4^\gamma(\widehat{G}_{\mathbf{k}_c}) = 2 - f_4^\gamma(\widehat{G}_{\mathbf{k}_c})$ . Therefore, the damping function  $f_4^\gamma(\widehat{G}_{\mathbf{k}_c})$  reads

$$f_4^\gamma(\widehat{G}_{\mathbf{k}_c}) = \frac{2H_4(\widehat{G}_{\mathbf{k}_c})}{1 + H_4(\widehat{G}_{\mathbf{k}_c})}. \quad (41)$$

In summary, the overall algorithm reads

---

#### Algorithm 1

---

- 1: Determine the overall damping from Eq.(40):  $H_4(\widehat{G}_{\mathbf{k}_c}) = \frac{2\nu\mathbf{k}_c^2 \hat{\omega}_{\mathbf{k}_c} \cdot \hat{\omega}_{\mathbf{k}_c}^*}{\hat{\omega}_{\mathbf{k}_c} \cdot \mathcal{C}(\boldsymbol{\omega}, \mathbf{u})_{\mathbf{k}_c}^* + \mathcal{C}(\boldsymbol{\omega}, \mathbf{u})_{\mathbf{k}_c} \cdot \hat{\omega}_{\mathbf{k}_c}^*}$
  - 2: Compute the damping function from Eq.(41):  $f_4^\gamma(\widehat{G}_{\mathbf{k}_c}) = 2H_4(\widehat{G}_{\mathbf{k}_c})/(1 + H_4(\widehat{G}_{\mathbf{k}_c}))$
  - 3: Construct the discrete filter,  $\widehat{G}_{\mathbf{k}}$ , with the requirement given in Eq.(36). The reader is referred to [36] for details.
  - 4: Solve the governing Eq. (27) using the formulae of  $f_4^\gamma(\widehat{G}_{\mathbf{k}})$  and  $h_4^\gamma(\widehat{G}_{\mathbf{k}})$  given in Eqs.(28) and (31), respectively.
- 

A similar reasoning can be applied in the physical space. Let us now consider an arbitrary part of the flow domain  $\Omega$  with periodic boundary conditions. Then, taking the  $L^2$  innerproduct of (1) with  $-\Delta\mathbf{u}$  leads to the enstrophy equation

$$\frac{1}{2} \frac{d}{dt} \|\boldsymbol{\omega}\|^2 = (\boldsymbol{\omega}, \mathcal{C}(\boldsymbol{\omega}, u)) - \nu \|\nabla\boldsymbol{\omega}\|^2, \quad (42)$$

where  $\|\boldsymbol{\omega}\|^2 = (\boldsymbol{\omega}, \boldsymbol{\omega})$  and the convective term contribution  $(\mathcal{C}(u, \boldsymbol{\omega}), \boldsymbol{\omega}) = 0$  vanishes because of the skew-symmetry (6) of the convective operator. Using the

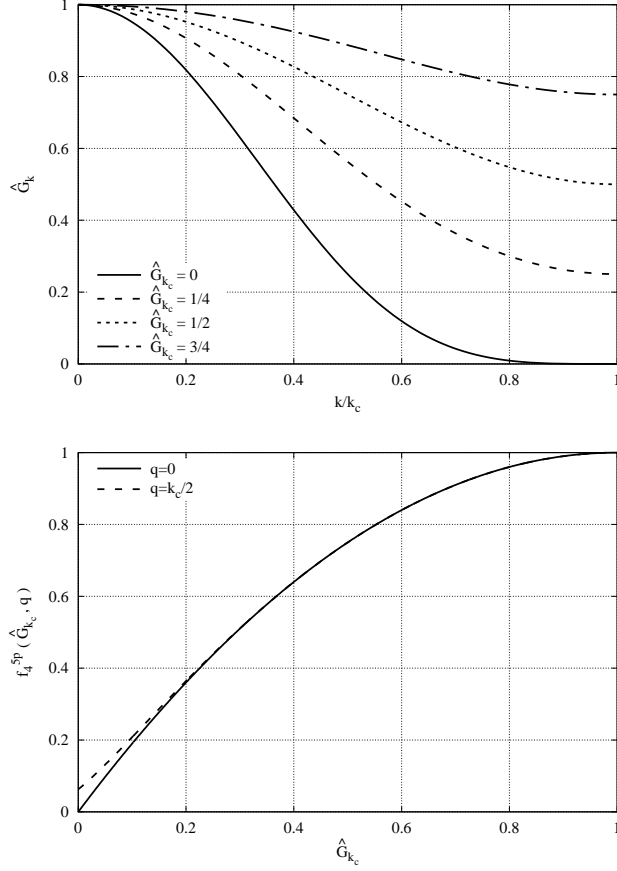


**Fig. 1** Top: transfer function of the 5-point filter given in Eq.(38) for different values of  $\hat{G}_{k_c}$ . Bottom: bandwidth for  $f_4^\gamma$  when using this 5-point filter.

results obtained by Chae [4] and following the same arguments as in [39], it can be shown that the vortex-stretching term can be expressed in terms of the third invariant of the rate-of-strain tensor,  $S(\mathbf{u})$ , *i.e.*  $R = 1/3 \text{tr}(S^3) = \det(S)$

$$(\boldsymbol{\omega}, \mathcal{C}(\boldsymbol{\omega}, \mathbf{u})) = \int_{\Omega} \boldsymbol{\omega} \cdot S\boldsymbol{\omega} = -\frac{4}{3} \int_{\Omega} \text{tr}(S^3) d\Omega = -4 \int_{\Omega} R d\Omega, \quad (43)$$

and the  $L^2(\Omega)$ -norm of  $\boldsymbol{\omega}$  in terms of the second invariant  $Q = -1/2 \text{tr}(S^2)$

$$\|\boldsymbol{\omega}\|^2 = -4 \int_{\Omega} Q d\Omega. \quad (44)$$

Then, recalling the Poincaré inequality the diffusive term can be bounded by

$$(\nabla \boldsymbol{\omega}, \nabla \boldsymbol{\omega}) = -(\boldsymbol{\omega}, \Delta \boldsymbol{\omega}) \leq -\lambda_{\Delta} (\boldsymbol{\omega}, \boldsymbol{\omega}), \quad (45)$$

where  $\lambda_{\Delta} < 0$  is the largest (smallest in absolute value) non-zero eigenvalue of the Laplacian operator  $\Delta$  on  $\Omega$ . If we now consider that the domain  $\Omega$  is a periodic box

of volume  $h$ , then  $\lambda_\Delta = -(\pi/h)^2$ . In a numerical simulation  $h$  would be related with the local grid size. Then, to prevent a local intensification of vorticity, *i.e.*  $\|\boldsymbol{\omega}\|_t \leq 0$ , the following inequality must be satisfied

$$H_4(\widehat{G}_{\mathbf{k}_c}) \frac{(\boldsymbol{\omega}, S\boldsymbol{\omega})}{(\boldsymbol{\omega}, \boldsymbol{\omega})} \leq -\nu\lambda_\Delta, \quad (46)$$

where, in this case (a 3D Cartesian grid),  $|\mathbf{k}_c| = \sqrt{3}\pi/h$ . This inequality is the analog to Eq.(40) in physical space. On the other hand, Rayleigh's principle states that

$$\max_{\boldsymbol{\omega} \neq 0} \frac{(\boldsymbol{\omega}, S\boldsymbol{\omega})}{(\boldsymbol{\omega}, \boldsymbol{\omega})} = \lambda_3, \quad (47)$$

therefore, it provides a lower bound for the damping function,  $H_4(\widehat{G}_{\mathbf{k}_c}) \leq \nu(-\lambda_\Delta/\lambda_3)$ . This was the approach considered in our previous work [37]. However, the maximum value is attained only if  $\boldsymbol{\omega}$  is aligned with the eigenvector corresponding to  $\lambda_3$ . This is not consistent with the preferential vorticity alignment with the intermediate eigenvector (see the works by Galanti *et al.* [11] and Dabbagh *et al.* [7]); therefore, the convective terms tends to be over-damped. This becomes especially relevant near walls. In order to overcome this drawback here we propose to rewrite the inequality (46) in terms of the invariants  $Q$  and  $R$ . From Eqs. (43)-(46) we deduce that  $H_4(\widehat{G}_{\mathbf{k}_c}) \leq \lambda_\Delta \nu Q/|R|$ , where the overall damping factor  $0 < H_4 \leq 1$ . Thus, a more proper definition of the overall damping factor at the smallest grid scale is given by

$$H_4(\widehat{G}_{\mathbf{k}_c}) = \min \{ \lambda_\Delta \nu Q/|R|, 1 \}. \quad (48)$$

### 3.3 On the determination of $\gamma$

A criterion to determine the damping function,  $f_4^\gamma(\widehat{G}_{\mathbf{k}_c})$ , at the smallest grid scale has been presented in the previous section. Then, the only parameter that still needs to be determined in Eq.(25) is the constant  $\gamma$ . As stated before, by simply setting  $\gamma = -1$ , the  $\mathcal{C}_4^\gamma$  becomes the sixth-order accurate  $\mathcal{C}_6$  regularization and the Galilean invariance is restored without introducing any additional modification in the dissipation term. However, the  $\mathcal{C}_6$  approximation itself suffers from a fundamental drawback. Namely, the overall method relies on the fact that Eq.(36) is approximately satisfied; therefore, the damping factor  $f_4^\gamma$  can be taken out of the summation in Eq. (35). This is not the case of  $f_6$ : notice that since  $\widehat{G}_0 = 1$ ,  $f_6(\widehat{G}_{\mathbf{k}_c}, \widehat{G}_{\mathbf{k}_c}, \widehat{G}_0) = 1$  irrespectively of the value of  $\widehat{G}_{\mathbf{k}_c}$ .

At this point, the 'optimal' value of  $\gamma$  could be determined by means of a trial-and-error numerical procedure. Alternatively, the constant  $\gamma$  can be obtained by assuming that the smallest grid scale  $k_c = |\mathbf{k}_c| = \sqrt{3}\pi/h$  lies within the inertial range for a classical Kolmogorov energy spectrum  $E(k) = C_K \varepsilon^{2/3} k^{-5/3}$ . In such a case, and recalling that  $\widehat{G}_{\mathbf{k}} = 1 - \alpha^2 |\mathbf{k}|^2 + \mathcal{O}(\alpha^4)$ , the total dissipation for  $k_T \leq k \leq k_c$  can be approximated by the contribution of the following two terms

$$\mathcal{D}_\nu \equiv \nu \int_{k_T}^{k_c} k^2 E(k) dk \quad \mathcal{D}_\nu'' \equiv \nu \int_{k_T}^{k_c} k^6 \alpha^4 E(k) dk, \quad (49)$$

where  $\mathcal{D}_\nu$  is the physical viscous dissipation and  $\mathcal{D}_\nu''$  is the additional dissipation introduced by the hyperviscosity term,  $(\mathcal{D}\mathbf{u}')'$ . Hence, integrating for a Kolmogorov energy spectrum, the total dissipation within the range  $k_T \leq k \leq k_c$  is given by

$$\mathcal{D}_\nu + \tilde{\gamma}\mathcal{D}_\nu'' = \frac{3\nu}{16}C_K\varepsilon^{2/3} \left\{ \left(4 + \tilde{\gamma}\alpha^4 k_c^4\right) k_c^{4/3} - \left(4 + \tilde{\gamma}\alpha^4 k_T^4\right) k_T^{4/3} \right\}, \quad (50)$$

where  $\tilde{\gamma} = 1/2(1 + \gamma)$  has been introduced here for the sake of simplicity. At the tail of the spectrum the following relation

$$\tilde{H}_4 \approx \frac{\mathcal{D}_\nu + \tilde{\gamma}\mathcal{D}_\nu''}{\varepsilon}, \quad (51)$$

represents the ratio between the total dissipation and the energy transferred from scales larger than  $k_T$  to the tail of the spectrum. Let us assume that  $\tilde{H}_4 = \mathcal{O}(H_4(\widehat{G}_{\mathbf{k}_c}))$  where the overall damping at the smallest grid scale,  $H_4(\widehat{G}_{\mathbf{k}_c})$ , is given by Eq.(48). However, at this point it is more suitable to express it in terms of the invariant  $Q$ . Recalling that the velocity field,  $\mathbf{u}$ , is solenoidal ( $\nabla \cdot \mathbf{u} = 0$ );  $\text{tr}(S) = 0$ , the characteristic equation of  $S$  reads

$$\det(\lambda I - S) = \lambda^3 + Q\lambda - R = 0. \quad (52)$$

Moreover, since  $S$  is a symmetric tensor all the eigenvalues are real-valued, *i.e.*  $\lambda_i \in \mathbb{R}$ ,  $i = 1, 2, 3$ . They are solutions of the characteristic equation (52); therefore, the discriminant of the cubic equation must be non-negative, *i.e.*  $-4Q^3 - 27R^2 \geq 0$ . Hence, the ratio  $|R|/Q$  can be bounded in terms of the invariant  $Q$ , *i.e.*  $0 \leq |R|/Q \leq \sqrt{-4Q/27}$ . Then, plugging this into Eq.(48) leads to

$$1 \geq H_4(\widehat{G}_\pi) \geq -\sqrt{\frac{27}{4}} \frac{\lambda_\Delta \nu}{\sqrt{-Q}}. \quad (53)$$

On the other hand, for a classical Kolmogorov energy spectrum, the ensemble averaged invariant  $Q$  is approximately given by

$$\langle Q \rangle = -\frac{1}{4} \int_0^{k_c} k^2 E(k) dk \approx -\frac{3}{16} C_K \varepsilon^{2/3} k_c^{4/3}. \quad (54)$$

Finally, combining Eqs.(53) and (54), the energy balance given by Eq.(51) results

$$\frac{-12\lambda_\Delta \nu \varepsilon}{\sqrt{C_K \varepsilon^{2/3} k_c^{4/3}}} \lesssim \mathcal{D}_\nu + \tilde{\gamma}\mathcal{D}_\nu''. \quad (55)$$

Then, plugging Eq.(50) and recalling that  $\lambda_\Delta = -3(\pi/h)^2$ ,  $k_c = \sqrt{3}\pi/h$  and  $\alpha \approx k_c^{-1}$ , the previous expression simplifies

$$1 \lesssim \frac{C_K^{3/2}}{32} \left\{ (4 + \tilde{\gamma}) - \left(4 + \tilde{\gamma} \left(\frac{k_T}{k_c}\right)^4\right) \left(\frac{k_T}{k_c}\right)^{4/3} \right\}. \quad (56)$$

Since  $k_c > k_T$  we can consider that  $4 \gg \tilde{\gamma}(k_T/k_c)^4$  to obtain a proper bound for  $\tilde{\gamma}$ ,

$$\tilde{\gamma} \gtrsim 4 \left\{ 8C_K^{-3/2} - \left(1 - \left(\frac{k_T}{k_c}\right)^{4/3}\right) \right\} \approx 4 \left(8C_K^{-3/2} - 1\right). \quad (57)$$

Hence, for a Kolmogorov constant of  $C_K \approx 1.58$  [9] it leads to a lower limit of  $\tilde{\gamma} \approx 12.1$  ( $\gamma \approx 23.2$ ). To confirm whether this is a proper estimation of  $\tilde{\gamma}$  numerical experiments are required. This is addressed in Section 4.

### 3.4 Blending regularization modeling and LES

The proposed  $\{\mathcal{CD}\}_4^\gamma$ -regularization can be straightforwardly applied for (pseudo) spectral methods. However, it may be quite cumbersome for other numerical methods such as finite volume, finite difference or finite element. In this context, it is worth mentioning the possibility to blend regularization modeling with an eddy-viscosity model for Large-Eddy Simulation (LES). Although they follow different arguments, the idea of blending both approaches has been already explored by Picano and Hanjalić [26] and Verstappen [40]. Shortly, LES equations result from applying a spatial commutative filter, with filter length  $\Delta$ , to the NS equations (1)

$$\partial_t \bar{\mathbf{u}} + \mathcal{C}(\bar{\mathbf{u}}, \bar{\mathbf{u}}) = \mathcal{D}\bar{\mathbf{u}} - \nabla \bar{p} - \nabla \cdot \tau(\bar{\mathbf{u}}), \quad \nabla \cdot \bar{\mathbf{u}} = 0, \quad (58)$$

where  $\bar{\mathbf{u}}$  is the filtered velocity and the subgrid stress tensor,  $\tau(\bar{\mathbf{u}})$ , aims to approximate the effect of the under-resolved scales, *i.e.*  $\tau(\bar{\mathbf{u}}) \approx \overline{\mathbf{u}} \otimes \bar{\mathbf{u}} - \bar{\mathbf{u}} \otimes \bar{\mathbf{u}}$ . Because of its inherent simplicity and robustness, the eddy-viscosity assumption is by far the most used closure model

$$\tau(\bar{\mathbf{u}}) \approx -2\nu_e S(\bar{\mathbf{u}}), \quad (59)$$

where  $\nu_e$  denotes the eddy-viscosity. This introduces a damping to the smallest grid scales that can be written as follows

$$H^{LES}(\widehat{G}_{\mathbf{k}_c}) = \min \{\nu/(\nu + \nu_e), 1\}. \quad (60)$$

There is an obvious analogy between this and the formula given in Eq.(48). Actually just rearranging terms leads to a variant of the *QR*-model proposed by Verstappen [39]

$$\nu_e = \lambda_\Delta^{-1} \frac{|R|}{Q} - \nu. \quad (61)$$

Furthermore, it is possible to use any other existing eddy-viscosity model to determine the overall damping,  $H_4(\widehat{G}_{\mathbf{k}_c})$ , by simply equating it to the overall damping  $H^{LES}(\widehat{G}_{\mathbf{k}_c})$  given in Eq.(60), *i.e.*  $H_4(\widehat{G}_{\mathbf{k}_c}) = H^{LES}(\widehat{G}_{\mathbf{k}_c})$ . Finally, it is possible to introduce the additional dissipation introduced by the hyperviscosity term via a modified eddy-viscosity,  $\tilde{\nu}_e$ , *i.e.*

$$1/h_4^\gamma(\widehat{G}_{\mathbf{k}_c}) = \min \{\nu/(\nu + \tilde{\nu}_e), 1\}, \quad (62)$$

where  $h_4^\gamma(\widehat{G}_{\mathbf{k}_c})$  follows from Eqs.(41) and (40). It must be noted that despite the amount of dissipation is the same, the hyperviscosity effect is actually lost when using an eddy-viscosity model. Finally, combining all these relations leads to  $\tilde{\nu}_e/\nu_e = 1/2$ . In summary, the overall algorithm reads

---

#### Algorithm 2

- 1: Determine  $\nu_e$  from an existing eddy-viscosity model, (*e.g.* Smagorinsky [30], WALE [22], QR [39], Sigma [23], S3PQR [31])...
  - 2: Determine the overall damping from Eq.(60):  $H_4(\widehat{G}_{\mathbf{k}_c}) = \min \{\nu/(\nu + \nu_e), 1\}$
  - 3: Compute the damping function from Eq.(41):  $f_4^\gamma(\widehat{G}_{\mathbf{k}_c}) = 2H_4(\widehat{G}_{\mathbf{k}_c})/(1 + H_4(\widehat{G}_{\mathbf{k}_c}))$
  - 4: Compute the modified eddy-viscosity:  $\tilde{\nu}_e = \nu_e/2$
-

Hence, this leads to a blending between regularization of the convective term and LES. Namely, instead of solving Eqs.(24), the new set of PDEs reads

$$\partial_t \mathbf{u}_\epsilon + \mathcal{C}_4^\gamma(\mathbf{u}_\epsilon, \mathbf{u}_\epsilon) = \mathcal{D}\mathbf{u}_\epsilon - \nabla p_\epsilon + \nabla \cdot (2\tilde{\nu}_e \mathcal{S}(\mathbf{u}_\epsilon)); \quad \nabla \cdot \mathbf{u}_\epsilon = 0, \quad (63)$$

where the modified eddy-viscosity,  $\tilde{\nu}_e$ , is obtained from the Algorithm 2.

#### 4 Numerical experiments

The  $\{\mathcal{CD}\}_4^\gamma$ -regularization has been proposed in the previous sections. In short, the original NS equations (1) are replaced by the smoother approximation given in Eqs.(24) where  $\mathcal{C}_4^\gamma(\mathbf{u}_\epsilon, \mathbf{u}_\epsilon)$  and  $\mathcal{D}_4^\gamma \mathbf{u}_\epsilon$  are given by Eqs.(20) and (25), respectively. Then, the criterion to determine the damping factor of the discrete linear filter at the smallest grid scale is given by Eq.(40). Finally, the value of  $\tilde{\gamma}$  has been approximately bounded by Eq.(57). In this section several numerical experiments are carried out to assess the performance of the proposed method outlined in Algorithm 1 and to check the adequacy of this bound.

Regarding the implementation of  $\mathcal{C}_4^\gamma(\mathbf{u}_\epsilon, \mathbf{u}_\epsilon)$ , it may be cumbersome because it implies (i) the calculation of  $\mathcal{C}_6$  given in Eq.(19) and (ii) the re-construction of discrete linear filters that fulfill the property given in Eq.(36). The latter is especially difficult since those filters should also be  $\gamma$ -dependent. Alternatively, we propose to re-use the discrete linear filters proposed in [36] for the  $\mathcal{C}_4$ -regularization. Hence, Eq.(28) needs simplification to be expressed in terms of  $f_4$  and not  $f_6$ . Recalling that  $f_6 \approx 1 - \alpha^6 |\mathbf{k}|^2 |\mathbf{p}|^2 |\mathbf{q}|^2$  and  $f_4 \approx 1 - \alpha^4 (|\mathbf{k}|^2 |\mathbf{p}|^2 + |\mathbf{k}|^2 |\mathbf{q}|^2 + |\mathbf{p}|^2 |\mathbf{q}|^2)$ , for a wide range of wavevectors we could simply assume that  $f_6 \approx 1$ . However, the foregoing analysis is localized at the smallest grid scale,  $\mathbf{k}_c$ , where this assumption is not correct. Therefore, hereafter we will simply consider that  $f_6 \approx f_4$ . In this case, the Eq. (41) that relates the damping function at the smallest grid scale,  $f_4^\gamma(\hat{G}_{\mathbf{k}_c})$ , with the overall damping,  $H_4(\hat{G}_{\mathbf{k}_c})$ , must be replaced by

$$f_4(\hat{G}_{\mathbf{k}_c}) = \frac{(1 + \tilde{\gamma})H_4(\hat{G}_{\mathbf{k}_c})}{1 + \tilde{\gamma}H_4(\hat{G}_{\mathbf{k}_c})}, \quad (64)$$

whereas  $h_4^\gamma(\hat{G}_{\mathbf{k}})$  is still given by Eq.(31).

##### 4.1 Burgers' equation

The numerical simulation of the 1D Burgers' equation

$$\partial_t u + \mathcal{C}(u, u) = \frac{1}{Re} \partial_{xx}^2 u + f, \quad (65)$$

on an interval  $x \in (0, 2\pi)$  with periodic boundary conditions has been chosen as a first test-case to assess the performance of the proposed  $\{\mathcal{CD}\}_4^\gamma$ -regularization method. Despite its simplicity, important aspects of the 3D NS equations remain (see [1], for instance). Note that now the convective term is given by  $\mathcal{C}(u, u) = u \partial_x u$ . In the Fourier space, it reads

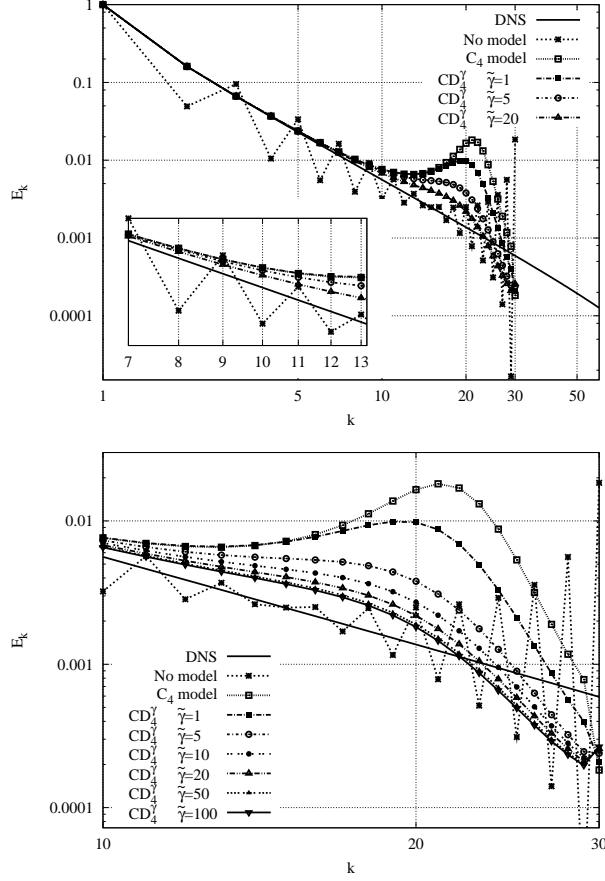
$$\partial_t \hat{u}_k + \sum_{p+q=k} \hat{u}_p i q \hat{u}_q = -\frac{k^2}{Re} \hat{u}_k + \hat{f}_k, \quad (66)$$

where  $\hat{u}_k(t)$  denotes the  $k$ -th Fourier mode of  $u(x, t) \in \mathbb{R}$ . The initial conditions are set to  $\hat{u}_k = k^{-1}$  whereas the forcing term vanishes  $\hat{f}_k = 0$  for  $k > 1$  and  $\hat{f}_1$  forces  $\partial_t \hat{u}_1 = 0$ . For details about the spectral numerical algorithm and the discrete linear filters the reader is referred to our previous work [36]. Results obtained at  $Re = 100$  with and without regularization for  $k_c = 30$  are displayed in Figure 2 and compared with the DNS reference solution (solid line) obtained with  $k_c = 300$ . Clearly, the direct simulation without model with  $k_c = 30$  is not able to capture the physics. At high wavenumbers, the energy is not dissipated enough; therefore, it is reflected back towards the larger scales. The zoom in Figure 2 (top) shows that the direct simulation with  $k_c = 30$  is substantially different from the DNS even for low wavenumbers. Regarding the effect of  $\tilde{\gamma}$ , different values have been tested. As expected, the  $\mathcal{C}_4$  solution, that corresponds to  $\tilde{\gamma} = 0$ , displays a hump at the tail of the spectrum. This effect was already observed in [36]. Figure 2 (bottom) shows how this undesirable effect tends to attenuate for increasing values of  $\tilde{\gamma}$ . Even more importantly, it seems to reach an asymptotic solution for  $\tilde{\gamma} \gtrsim 100$ . This is in a fairly good agreement with the estimation given by Eq.(57). Notice that for the Burgers' equation  $C_K \approx 0.452$ ; therefore, it leads to  $\tilde{\gamma} \gtrsim 101.3$ . Similar results are obtained for  $Re = 200$  (see Figure 3). In this case, the DNS reference solution has been computed with  $k_c = 600$ . Again the full spectrum of the DNS solution is not depicted for the sake of clarity. As expected, in this case the hump at the tail of the spectrum of the  $\mathcal{C}_4$  solution is even more evident. Then, the numerical solution is asymptotically improved for successively higher values of  $\tilde{\gamma}$  until  $\tilde{\gamma} = 100$  (see Figure 3, bottom). Regarding the dependence with the numerical resolution, Figure 4 displays the numerical solutions for both  $Re$ -numbers and different values of  $k_c$ . It must be noted that a small pile-up of energy at the smallest scale,  $k_c$ , is observed. This spurious effect is due to the fact that the overall damping effect in Eq.(40) has been derived for the semi-discrete equations, *i.e.* without considering the time-integration scheme. In this way, the energy at the highest mode is still able to grow. This issue was already noticed in [19] where  $\mathcal{C}_4$ -regularization was tested for a Burgers' equation using an explicit first-order Euler scheme. An appropriate modification of Eq.(40) would be necessary to remove this spurious effect accordingly to the time-integration scheme. Practically, this modification has a negligible effect to the rest of scales and makes the algorithm unnecessarily complicated. For these reasons, in this work we decided not to include this modification.

#### 4.2 Forced homogeneous isotropic turbulence

The numerical simulation of forced homogeneous isotropic turbulence has been chosen as the second test-case. In this case, the governing equations are solved with a pseudo-spectral code using the classical 3/2 dealiasing rule and an explicit second-order Adams-Bashforth scheme is used for time-integration. Filters proposed in our previous work [36] are applied in the spectral space. The total amount of energy in the first two modes is kept constant following the approach proposed in [5].

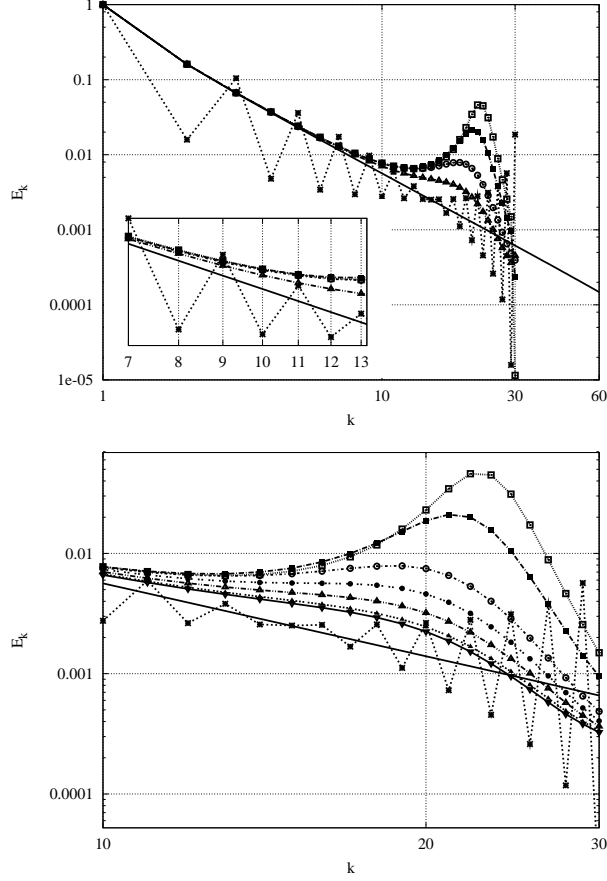
Firstly, the Taylor micro-scale Reynolds number is set to  $Re_\lambda \approx 72$ . Figure 5 (top) displays the results for a box size of  $16^3$  for different values of  $\tilde{\gamma}$  from 0 up to 30. Results without model are shown for box size of  $32^3$  (the simulation is unstable



**Fig. 2** Top: energy spectra of the steady-state solution of the Burgers' equation at  $Re = 100$  with and without modeling, for  $k_c = 30$ . Direct comparison with the DNS reference solution (solid line) with  $k_c = 300$ . Bottom: zoom of the tail of the spectra for different values of  $\tilde{\gamma}$  from 0 to 100.

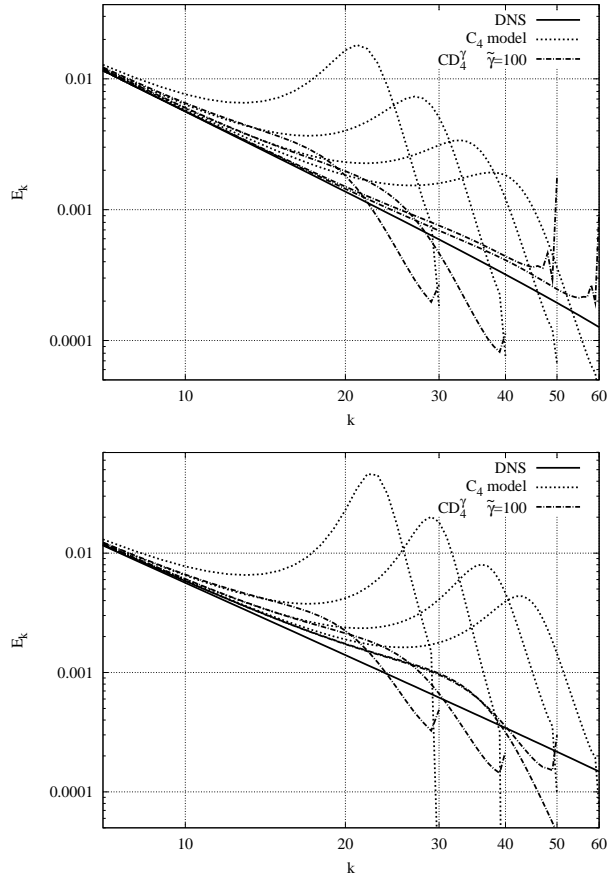
for  $16^3$  due to the fact that the pseudo-spectral convective operator is not skew-symmetric and hence strict conservation of kinetic energy is not guaranteed [2]). As expected, the original hump displayed for  $\tilde{\gamma} = 0$  attenuates for increasing values of  $\tilde{\gamma}$ . Moreover, the lower bound for  $\tilde{\gamma}$  given by Eq.(57) is in a fairly good agreement with these numerical tests. Even more importantly, for  $\tilde{\gamma}$  bigger than a certain value, the results are virtually independent on the value of  $\tilde{\gamma}$ .

Figure 5 (bottom) displays LES results obtained for a box size of  $64^3$  at  $Re_\lambda \approx 202$  together with results without model using a box size of  $256^3$ . In this case, the energy-containing and dissipative scales are clearly separated by an inertial range. Again, the hump at the tail of the spectrum attenuates for increasing values of  $\tilde{\gamma}$ . More importantly, the inertial range is well predicted only for those cases with  $\tilde{\gamma} \gtrsim 14$ , in relatively good agreement with the lower bound given by Eq.(57). Finally, to assess the validity of Algorithm 2, where the blending between regularization modeling and LES is proposed, the same test-case has been



**Fig. 3** Top: energy spectra of the steady-state solution of the Burgers' equation at  $Re = 200$  with and without modeling, for  $k_c = 30$ . Direct comparison with the DNS reference solution (solid line) with  $k_c = 600$ . Bottom: zoom of the tail of the spectra for different values of  $\tilde{\gamma}$  from 0 to 100. The legend is the same as in Figure 2.

solved using this approach. Results are shown in Figure 6 together with the results obtained using a pure LES (denoted as *LES*). The difference between both approaches is that in the pure LES the convective term is not regularized and the value for the eddy-viscosity is  $\nu_e$  instead of  $\tilde{\nu}_e$  (see Algorithm 2). It is observed that the proposed approach (denoted as  $C_4^\gamma + LES$  in Figure 6) has a positive impact in the results: the excess of energy in the inertial range decreases despite the lower dissipation introduced by the eddy-viscosity model. This effect is attributed to the fact that the regularization of the non-linear convective term reduces the dynamical complexity of the original NS equations.



**Fig. 4** Energy spectra of the steady-state solution of the Burgers' equation at  $Re = 100$  (top) and  $Re = 200$  (bottom) with  $\mathcal{C}_4$  and  $\{\mathcal{CD}\}_4^{\gamma=100}$  for  $k_c = 30, 40, 50$  and  $60$ . Direct comparisons with the DNS reference solution (solid lines).

#### 4.3 Turbulent channel flow

To test the performance of the proposed model with the presence of walls, a turbulent channel flow has been considered. In this case, the code is based on a fourth-order symmetry-preserving finite volume discretization [41] of the incompressible NS equations on structured staggered grids. A second-order self-adapting explicit scheme [34] is used for the time integration and the pressure-velocity coupling is solved by means of a classical fractional step projection method. For details about the numerical algorithms and the verification of this code the reader is referred to Gorobets *et al.* [14].

Both previous test-cases were solved using a (pseudo) spectral method where the  $\{\mathcal{CD}\}_4^{\gamma}$ -regularization can be easily applied. However, as mentioned in Section 3.4, it may be quite cumbersome for a finite volume method. Therefore, in this case, we use the blending between regularization modeling and LES (see Al-

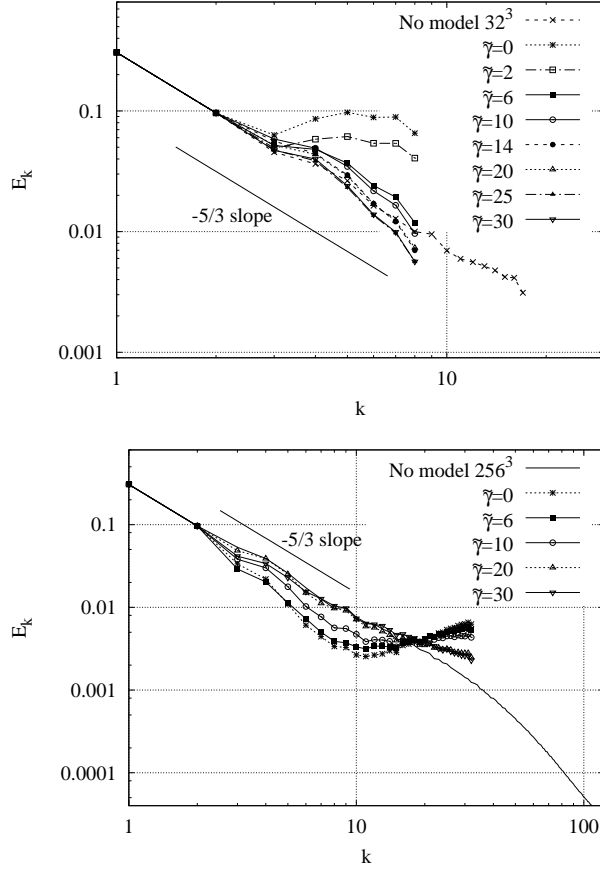


**Fig. 5** Three-dimensional energy spectra at  $Re_\lambda \approx 72$  (top) and  $Re_\lambda \approx 202$  (bottom) for different values of  $\tilde{\gamma}$  from 0 up to 30.

gorithm 2 in Section 3.4). In this regard, the eddy-viscosity,  $\nu_e$ , is computed using the  $S3QR$ -model recently proposed by Trias *et al.* [31]. Namely,

$$\nu_e^{S3QR} = (C_{s3qr}\Delta)^2 Q_{GG^T}^{-1} R_{GG^T}^{5/6}, \quad (67)$$

where  $C_{s3qr} = 0.762$ ,  $Q_{GG^T}$  and  $R_{GG^T}$  are the second and third invariants of the symmetric second-order tensor  $GG^T$  and  $G$  is the gradient of the resolved velocity field, *i.e.*  $G \equiv \nabla \bar{\mathbf{u}}$ . Likewise the Vreman's model [42], it is also based on the invariants of the second-order tensor  $GG^T$ . However, it has the proper cubic near-wall behavior. Apart from this, it fulfills a set of desirable properties (positiveness, locality, Galilean invariance, and automatically switches off for laminar, 2D, and axisymmetric flows), it is well-conditioned, has a low computational cost and no intrinsic limitations for statistically inhomogeneous flows. Moreover, regarding the spatial discretization of the eddy-viscosity model, the approach proposed by Trias *et al.* [32] has been used.

Figures 7 and 8 show the performance of the proposed approach for a turbulent channel flow at  $Re_\tau \approx 395$  (a Reynolds number of  $Re_b = 13760$  based on the

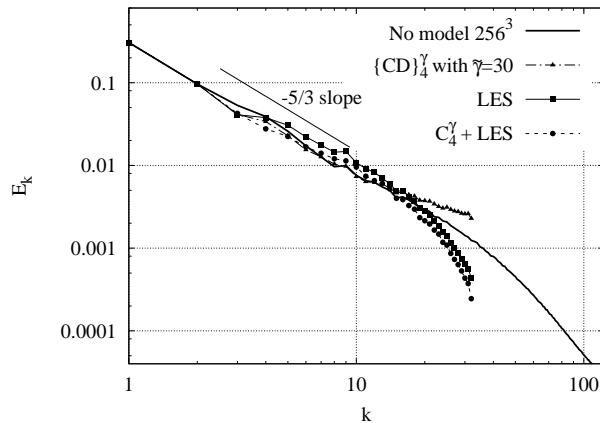


**Fig. 6** Three-dimensional energy spectra at  $Re_\lambda \approx 202$  for both the blending between regularization and LES (denoted as  $C_4^\gamma + LES$ ) proposed in Section 3.4 and a pure LES (denoted as  $LES$ ). Results denoted as  $\{CD\}_4^\gamma$  correspond to the simulation shown in Figure 5 (bottom) with  $\tilde{\gamma} = 30$ .

channel width and the bulk velocity is imposed for all the simulations). The results are compared with the DNS data of Moser *et al.* [21]. The dimensions of the channel are taken equal to those of the DNS, *i.e.*  $2\pi \times 2 \times \pi$ . The computational grid is reduced in a significant manner; namely, the DNS was performed on a  $256 \times 193 \times 192$  grid whereas the modeled results have been obtained with a  $32^3$  mesh, *i.e.* the DNS used about 290 times more grid points than the present simulations. They are uniformly distributed in the stream-wise and the span-wise directions whereas the wall-normal points are distributed using a piece-wise hyperbolic sine functions. For lower-half of the channel the distribution of points is given by

$$y_j = \sinh(\gamma j / N_y) / \sinh(\gamma / 2) \quad j = 0, 1, \dots, N_y / 2, \quad (68)$$

where  $N_y$  denotes the number of grid points in the wall-normal direction. The stretching parameter,  $\gamma$ , is taken equal to 7. Then, the grid points in the upper-half are computed by means of symmetry. With this distribution and  $N_y = 32$ , the first off-wall grid point is located at  $y^+ \approx 2.6$ , *i.e.* inside the viscous sublayer ( $y^+ < 5$ ). In this case, the subgrid characteristic length is computed as the cube root of the cell volume, *i.e.*  $\Delta \equiv (\Delta x \Delta y \Delta z)^{1/3}$ . Averages over the four statistically invariant transformations (time, stream-wise and span-wise directions and central plane symmetry) are carried out for all the fields. The standard notation  $\langle \cdot \rangle$  is used to denote this averaging procedure. The averaging over time starts after a start-up period. This period as well as the time-span over which the results are averaged, 60 time-units (based on the skin friction velocity,  $u_\tau$ , and the channel width), are identical for all the simulations presented here.

The results displayed in Figure 7 are in good agreement with the DNS data. To illustrate the contribution of the model in improving the quality of the solution, the results obtained with a  $96^3$  mesh without model, *i.e.*  $\nu_e = 0$ , are also shown. Moreover, to study the effect of the regularization of the convective term, results are also compared with a pure LES using the same mesh. That is, results

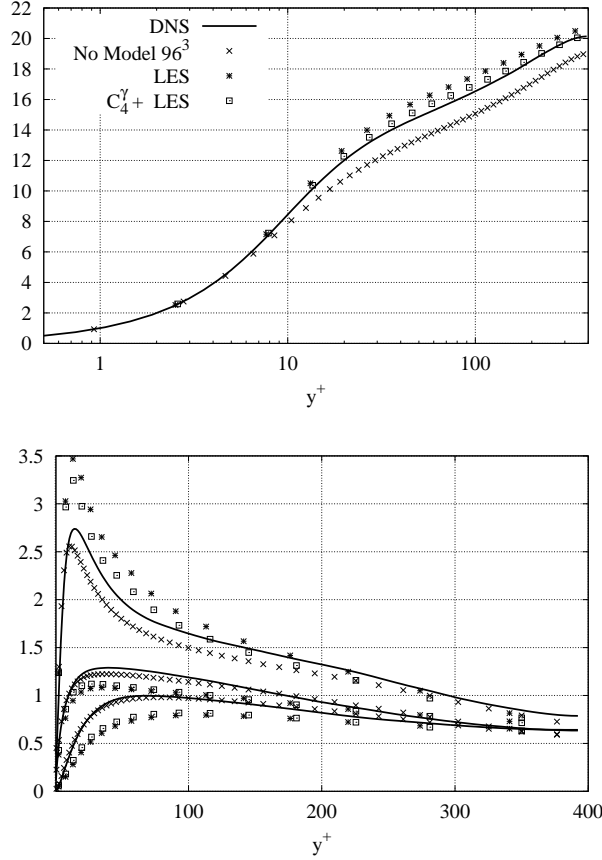


**Fig. 7** Results for a turbulent channel flow at  $Re_\tau \approx 395$  obtained with a  $32^3$  mesh for both the blending between regularization and LES (denoted as  $C_4^\gamma + LES$ ) proposed in Section 3.4 and a pure LES (denoted as  $LES$ ). Solid line corresponds to the DNS by Moser *et al.* [21] and crosses correspond to a  $96^3$  mesh without model, *i.e.*  $\nu_e = 0$ . Top: average stream-wise velocity,  $\langle u \rangle$ . Bottom: root-mean-square of the fluctuating velocity components (from top to bottom,  $u_{rms}$ ,  $w_{rms}$  and  $v_{rms}$ , respectively.)

denoted as  $C_4^\gamma + LES$  in Figure 7 have been obtained by solving Eq.(63) using the Algorithm 2 whereas pure LES results (denoted as  $LES$ ) have been obtained by solving the LES equations (58). Therefore, differences of the latter approach respect to the former are twofold: the convective term is not altered (smoothed) and the value for the eddy-viscosity is  $\nu_e$  instead of  $\tilde{\nu}_e$  (see Algorithm 2). The proposed approach has a positive impact for both the mean flow solution and the turbulent statistics. Regarding the mean flow (see Figure 7, top), the solution is significantly improved in those regions where the model is really switch on, *i.e.* the buffer layer ( $5 < y^+ < 30$ ) and the log-law region ( $y^+ > 30$ ), whereas the quality of the solutions in the viscous sublayer ( $y^+ < 5$ ) is very similar for all simulations due to the rescaling in wall-units. Results for the root-mean-square of the fluctuating velocity components (see Figure 7, bottom) are also improved for

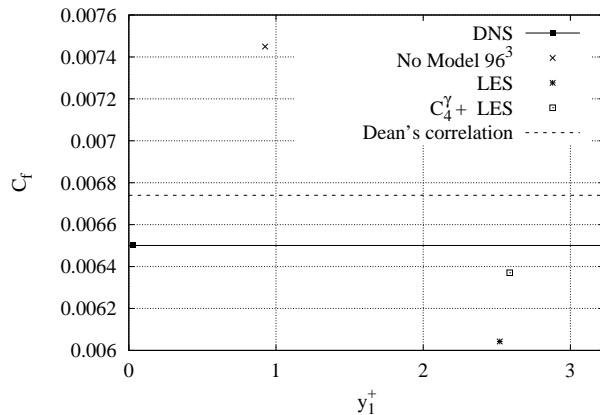


**Fig. 8** Skin friction coefficient,  $C_f$ , versus the position of the first off-wall grid point in wall-units,  $y_1^+$ . Results correspond to the same simulations as in Figure 7. In this case, the skin friction obtained with the Dean’s correlation  $C_f = 0.073Re_b^{-1/4} = 0.00674$  [8], is shown for comparison.

all three components. In this regard, the most relevant improvement corresponds to the stream-wise velocity fluctuations: they are slightly damped compared with the pure LES solution getting closer to the DNS reference data. Only minor differences are observed for the span-wise and wall-normal velocity fluctuations: both are slightly increased in the buffer layer and in the first part of the log-law region. Finally, results of the skin friction coefficient,  $C_f$ , versus the position of the first off-wall grid point are displayed in Figure 8. It is remarkable that the results obtained without modeling are quite far off the DNS solution despite having the first grid point at  $y_1^+ \lesssim 1$ . Using a mesh that it is three times coarser, models are able to improve the prediction of  $C_f$ , being the proposed approach ( $C_4^\gamma + LES$ ) significantly more accurate than a simple LES. It is important to note that for a given mesh the proposed approach has a lower computational cost. Despite the computation of  $C_4^\gamma$  in Eq.(63) implies an additional cost (around 10%), this is compensated by the significant reduction of the number of time-steps to complete the simulation. This reduction of the total number of time-steps is mainly due to the fact that larger time-steps can be used because the actual values of the turbulent viscosity are smaller for the blended approach.

## 5 Concluding remarks and future research

Since DNS simulations are not feasible for real-world applications, the  $\{CD\}_4^\gamma$ -regularization of the NS equations has been proposed as a simulation shortcut: the convective and diffusive operators in the NS equations (1) are replaced by the  $\mathcal{O}(\epsilon^4)$ -accurate smooth approximation given by Eq.(20) and Eq.(25), respectively. The symmetries and conservation properties of the original convective term are exactly preserved. Doing so, the production of smaller and smaller scales of motion is restrained in an unconditionally stable manner. In this way, the new set of

equations is dynamically less complex than the original NS equations, and therefore more amenable to be numerically solved. The only additional ingredient is a self-adjoint linear filter whose local filter length is determined from the requirement that vortex-stretching must be stopped at the scale set by the grid. This can be easily satisfied in spectral space via Eq.(40) provided that discrete filter satisfies Eq.(36), *i.e.* the triadic interactions at the smallest scale are virtually independent of the interacting pairs. This was addressed in detail in a previous work [36]. However, in physical space it becomes more cumbersome. To circumvent this, a blending approach between the regularization of the non-linear convective term and eddy-viscosity model for LES has been proposed.

In the present paper, the parameter  $\gamma$  of Eq.(24) has been approximately bounded by assuming a Kolmogorov energy spectrum. This has been addressed in Section 3.3 where the following bound has been determined:

$$\tilde{\gamma} \gtrsim 4 \left( 8C_K^{-3/2} - 1 \right), \quad (69)$$

where  $\tilde{\gamma} = 1/2(1 + \gamma)$  and  $C_K$  is the Kolmogorov constant. Simulations for a 1D Burgers' equation and for homogeneous isotropic turbulence at different Reynolds numbers seem to confirm the adequacy of the bound given by Eq.(69). In this way, the proposed method constitutes a parameter-free turbulence model. Apart from this, the above-mentioned blending approach between regularization and LES have been successfully tested for a turbulent channel flow. To do so, the recently proposed S3QR-model [31] has been used to compute the eddy-viscosity. Hence, the list of desirable properties (positiveness, locality, Galilean invariance, proper near-wall behavior, and automatically switches off for laminar, 2D, and axisymmetric flows) of the S3QR model are inherited by the blending approach proposed here. Therefore, the overall approach seems to be well suited for engineering applications. In this regard, several issues may significantly affect their performance. The proper calculation of the subgrid characteristic length on unstructured grids or the (global dynamic?) determination of model constant are examples thereof. All these issues are part of our future research plans to test these models for complex flows.

**Acknowledgements** This work has been financially supported by the *Ministerio de Economía y Competitividad*, Spain (ENE2017-88697-R) and a *Ramón y Cajal* postdoctoral contract (RYC-2012-11996). Calculations have been performed on the IBM MareNostrum supercomputer at the Barcelona Supercomputing Center. The authors thankfully acknowledge these institutions.

## References

1. Basu, S.: Can the dynamic eddy-viscosity class of subgrid-scale models capture inertial-range properties of Burgers turbulence? *Journal of Turbulence* **10**(12), 1–16 (2009)
2. Capuano, F., Coppola, G., Balarac, G., de Luca, L.: Energy preserving turbulent simulations at a reduced computational cost. *Journal of Computational Physics* **298**, 480–494 (2015)
3. Carati, D., Winckelmans, G.S., Jeanmart, H.: Exact expansions for filtered-scales modelling with a wide class of LES filters. In: *Direct and Large-Eddy Simulation III*, pp. 213–224. Kluwer (1999)

4. Chae, D.: On the spectral dynamics of the deformation tensor and a new a priori estimates for the 3D Euler equations. *Communications in Mathematical Physics* **263**, 789–801 (2005)
5. Chen, S., Doolen, G.D., Kraichnan, R.H., She, Z.: On statistical correlations between velocity increments and locally averaged dissipation in homogeneous turbulence. *Physics of Fluids A* **5**, 458 (1993)
6. Cheskidov, A., Holm, D.D., Olson, E., Titi, E.S.: On a Leray- $\alpha$  model of turbulence. *Proceedings of the Royal Society A: Mathematical, Physical and Engineering Sciences* **461**(2055), 629–649 (2005)
7. Dabbagh, F., Trias, F.X., Gorobets, A., Oliva, A.: On the evolution of flow topology in turbulent Rayleigh–Bénard convection. *Physics of Fluids* **28**, 115,105 (2016)
8. Dean, R.B.: Reynolds number dependence of skin friction and other bulk flow variables in two-dimensional rectangular duct flow. *Journal of Fluids Engineering, Transactions of the ASME* **100**(2), 215–223 (1978)
9. Donzis, D.A., Sreenivasan, K.R.: The bottleneck effect and the Kolmogorov constant in isotropic turbulence. *Journal of Fluid Mechanics* **657**, 171–188 (2010)
10. Foias, C., Holm, D.D., Titi, E.S.: The Navier-Stokes-alpha model for fluid turbulence. *Physica D* **152**, 505–519 (2001)
11. Galanti, B., Gibbon, J., Heritage, M.: Vorticity alignment results for the three-dimensional Euler and Navier-Stokes equations. *Nonlinearity* **10**(6), 1675–1694 (1997)
12. Geurts, B.J., Holm, D.D.: Regularization modeling for large-eddy simulation. *Physics of Fluids* **15**, L13–L16 (2003)
13. Geurts, B.J., Holm, D.D.: Leray and LANS- $\alpha$  modelling of turbulent mixing. *Journal of Turbulence* **7**, 1–33 (2006)
14. Gorobets, A., Trias, F.X., Soria, M., Oliva, A.: A scalable parallel Poisson solver for three-dimensional problems with one periodic direction. *Computers & Fluids* **39**, 525–538 (2010)
15. Graham, J.P., Holm, D.D., Mininni, P., Pouquet, A.: The effect of subfilter-scale physics on regularization models. *Journal of Scientific Computing* **49**(1), 21–34 (2011)
16. Guermond, J.L., Oden, J.T., Prudhomme, S.: An interpretation of the Navier-Stokes-alpha model as a frame-indifferent Leray regularization. *Physica D* **177**, 23–30 (2003)
17. Guermond, J.L., Oden, J.T., Prudhomme, S.: Mathematical perspectives on large eddy simulation models for turbulent flows. *Journal of Mathematical Fluid Mechanics* **6**, 194–248 (2004)
18. Guermond, J.L., Prudhomme, S.: On the construction of suitable solutions to the Navier-Stokes equations and questions regarding the definition of large-eddy simulations. *Physica D* **207**, 64–78 (2005)
19. Helder, J., Verstappen, R.: On restraining convective subgrid-scale production in Burgers’ equation. *International Journal for Numerical Methods in Fluids* **56**(8), 1289–1295 (2008)
20. Leray, J.: Sur le mouvement d’un liquide visqueux emplissant l’espace. *Acta Mathematica* **63**, 193–248 (1934)
21. Moser, R.D., Kim, J., Mansour, N.N.: Direct numerical simulation of turbulent channel flow up to  $Re_\tau = 590$ . *Physics of Fluids* **11**, 943–945 (1999)
22. Nicoud, F., Ducros, F.: Subgrid-scale stress modelling based on the square of the velocity gradient tensor. *Flow, Turbulence and Combustion* **62**(3), 183–200 (1999)
23. Nicoud, F., Toda, H.B., Cabrit, O., Bose, S., Lee, J.: Using singular values to build a subgrid-scale model for large eddy simulations. *Physics of Fluids* **23**(8), 085,106 (2011)
24. Norgard, G., Mohseni, K.: A regularization of the Burgers equation using a filtered convective velocity. *Journal of Physics A: Mathematical and Theoretical* **41**(34) (2008). DOI 10.1088/1751-8113/41/34/344016
25. Perot, J.B.: Discrete conservation properties of unstructured mesh schemes. *Annual Review of Fluid Mechanics* **43**, 299–318 (2011)
26. Picano, F., Hanjalić, K.: Leray- $\alpha$  regularization of the Smagorinsky-closed filtered equations for turbulent jets at high Reynolds numbers. *Flow, Turbulence and Combustion* **89**(4), 627–650 (2012)
27. Pope, S.B.: *Turbulent Flows*. Cambridge University Press (2000)
28. van Reeuwijk, M., Jonker, H.J.J., Hanjalić, K.: Incompressibility of the Leray- $\alpha$  model for wall-bounded flows. *Physics of Fluids* **18**(1), 018103 (2006)
29. van Reeuwijk, M., Jonker, H.J.J., Hanjalić, K.: Leray- $\alpha$  simulations of wall-bounded turbulent flows. *International Journal of Heat and Fluid Flow* **30**(6), 1044 – 1053 (2009)
30. Smagorinsky, J.: General Circulation Experiments with the Primitive Equations. *Monthly Weather Review* **91**, 99–164 (1963)

31. Trias, F.X., Folch, D., Gorobets, A., Oliva, A.: Building proper invariants for eddy-viscosity subgrid-scale models. *Physics of Fluids* **27**(6), 065,103 (2015)
32. Trias, F.X., Gorobets, A., Oliva, A.: A simple approach to discretize the viscous term with spatially varying (eddy-)viscosity. *Journal of Computational Physics* **253**, 405–417 (2013)
33. Trias, F.X., Gorobets, A., Pérez-Segarra, C.D., Oliva, A.: DNS and regularization modeling of a turbulent differentially heated cavity of aspect ratio 5. *International Journal of Heat and Mass Transfer* **57**, 171–182 (2013)
34. Trias, F.X., O. Lehmkuhl: A self-adaptive strategy for the time-integration of Navier-Stokes equations. *Numerical Heat Transfer, part B* **60**(2), 116–134 (2011)
35. Trias, F.X., O. Lehmkuhl, A. Oliva, C.D. Pérez-Segarra, R.W.C.P. Verstappen: Symmetry-preserving discretization of Navier-Stokes equations on collocated unstructured meshes. *Journal of Computational Physics* **258**, 246–267 (2014)
36. Trias, F.X., Verstappen, R.W.C.P.: On the construction of discrete filters for symmetry-preserving regularization models. *Computers & Fluids* **40**, 139–148 (2011)
37. Trias, F.X., Verstappen, R.W.C.P., Gorobets, A., Soria, M., Oliva, A.: Parameter-free symmetry-preserving regularization modeling of a turbulent differentially heated cavity. *Computers & Fluids* **39**, 1815–1831 (2010)
38. Verstappen, R.: On restraining the production of small scales of motion in a turbulent channel flow. *Computers & Fluids* **37**, 887–897 (2008)
39. Verstappen, R.: When does eddy viscosity damp subfilter scales sufficiently? *Journal of Scientific Computing* **49**(1), 94–110 (2011)
40. Verstappen, R.: Blended scale-separation models for large eddy simulations. In: 14<sup>th</sup> European Turbulence Conference. Lyon, France (2013)
41. Verstappen, R.W.C.P., Veldman, A.E.P.: Symmetry-Preserving Discretization of Turbulent Flow. *Journal of Computational Physics* **187**, 343–368 (2003)
42. Vreman, A.W.: An eddy-viscosity subgrid-scale model for turbulent shear flow: Algebraic theory and applications. *Physics of Fluids* **16**(10), 3670–3681 (2004)